# Effect of Stress−Structure Coupling on the Rheology of Complex Fluids: Poor Polymer Solutions

**Jan W. van Egmond**

*Department of Chemical Engineering, University of Massachusetts, Amherst, Massachusetts 01003*

*Received May 16, 1997; Revised Manuscript Received September 8, 1997*[⊗]

ABSTRACT: When sheared, near-$\theta$ polymer solutions undergo a dramatic enhancement of concentration fluctuations due to a coupling between polymer stress and concentration. This phenomenon is easily observed as an increase in turbidity. The flow-induced mesoscopic structure is, however, anisotropic and results in an extra "anomalous" stress in the fluid. The dynamics and rheology of such a system is discussed and a phenomenological description for stress evolution as a result of concentration fluctuation enhancement is developed. The rheological properties are shown to be quite unusual and include a shear thickening regime and the appearance of a second overshoot on flow startup. The methodology developed in this paper can be applied to a large number of problems involving flow-modified structure in complex fluids. An approximate stress−optic rule for the anomalous stress is developed and predictions for simple shear flow are compared with experimental results.

## I. Introduction

In recent years, mesoscopic structural changes in polymer solutions induced by applied flow fields have attracted much attention in the literature.[1,2] The first such reports concerned the dramatic increase in turbidity induced in polymer solutions by rapid shearing at temperatures above the quiescent cloud point.[3] A theoretical model to explain this phenomenon, sometimes known as flow-induced phase separation, was introduced by Wolf and co-workers.[4] This model is based on the inclusion of chain deformation in the Flory−Huggins free energy of mixing, and while it predicts both shear-induced mixing and demixing, it is a macroscopic, equilibrium model and as such cannot predict the dynamics and structure of concentration fluctuations. The mechanism behind flow-induced turbidity is the coupling of stress relaxation and diffusion of concentration fluctuations as described by the two-fluid model developed by Brochard and de Gennes[5] and verified by Adam and Delsanti[6] with dynamic light scattering experiments in entangled polymer solutions of poor quality. The more recent theoretical models by Helfand and Fredrickson[7] (HF), Onuki and Doi,[8,9] and Milner[10] that address the mechanism for stress enhancement of concentration fluctuations have successfully predicted many of the static and dynamic aspects of the phenomenon. This HF mechanism is due to a coupling between concentration fluctuations and local polymer stress and leads to the enhancement of concentration fluctuations along preferred directions. Experimental studies measuring flow-induced anisotropy of concentration fluctuations under flow have recently been undertaken by several groups.[11−30] For example, small angle light scattering experiments[12−14] revealed highly anisotropic scattering ("butterfly") patterns that were in qualitative agreement with the HF model. These experiments were conducted on entangled solutions of polystyrene (PS) in dioctyl phthalate (DOP), a system that has since become a standard in this type of study. At low shear rates, experiment and theory agree in that the axis along which scattering is highest is approximately parallel to the polymer stress axis. Milner[31] and Ji and Helfand[32] have developed more sophisticated models that feature a coupled set of Langevin equations for polymer concentration, momentum, and polymer strain. Inclusion of a polymer stress relaxation time in these theories results in the appearance of a wavenumber $k_c$, at which the symmetric scattering peaks of the observed butterfly patterns appear. This wavenumber corresponds to a crossover between the relaxation times of stress and concentration diffusion and was first introduced by de Gennes and Brochard.[33,5]

Much of the recent work has focused on predicting and measuring the structure and anisotropy of stress-enhanced concentration fluctuations. Such structural changes should also result in corresponding changes in viscosity and other rheological parameters. In addition to the polymeric stresses attributed to molecular conformational anisotropy in flowing polymeric fluids, long-lived concentration fluctuations also contribute to the overall stress when their distribution becomes anisotropic. The latter contribution, known as the anomalous or critical stress, becomes significant when fluctuations become highly interactive with stress. For a poor polymer solution this is in the pretransitional region near a phase boundary where osmotic forces are weak and fluctuations long lived. The anomalous stress was first investigated in the context of sheared simple fluids in the vicinity of the critical point by Fixman and Sallavanti,[34,35] Yamada and Kawasaki,[36] Oxtoby,[37] and Onuki.[38] The contribution of the anomalous stress to the linear viscoelastic properties in blends and block copolymer mesophases has been considered by Fredrickson and Larson[39,40] and Onuki.[41] These theories have been used to predict the zero shear viscosity near the critical point and include contributions to fluctuation dynamics from convection and diffusion but not from the stress-enhancement mechanism. Recently, this treatment has been extended to the linear viscoelastic properties of polymer blends.[42,43] In the homogeneous regime near phase separation of PS/PVME blends it was found that time−temperature superposition failed at time scales longer than those corresponding to single chain relaxation. This failure was related to the collective motion of several chains in regions rich in PS through the enhancement of concentration fluctuations.[43]

[⊗] Abstract published in *Advance ACS Abstracts,* November 15, 1997.

S0024-9297(97)00689-X CCC: $14.00 

Polymer solutions are usually shear thinning at high shear rates. Many solutions also display a shear-thickening regime following shear thinning, especially when the polymer is of high molecular weight and shear rates are high or solvent quality is poor. These include polyisobutylene solutions,[44] polyethylene oxide (PEO) in water, PS in decalin,[45] polyethylene in xylene, polypropylene in tetralin, and PEO in ethanol.[46] Subsequently, the formation of intermolecular associations or flow-induced structures has been shown to be the underlying mechanism responsible for shear thickening in dilute solutions of high molecular weight.[46−48] More recently, Dupuis *et al.*[49] have used mechanical rheology to study the effect of aggregate formation on shear thickening and instability in polyacrylamide solutions. Brownian dynamics simulations have also provided confirmation on the role of associations in shear thickening in dilute solutions.[50] Semidilute PS/DOP solutions also display a shear-thickening regime at high shear rates.[11,18,27] Yanase *et al.*[11] observed that the onset of shear thickening is at shear rates when scattering dichroism becomes very large and positive, implying that concentrated regions are elongated along the flow direction. There are other phenomena related to structural changes that show strong connections with the shear-thickening regime and include overshoots and large fluctuations in scattering dichroism and scattering intensity.[11,30] Using birefringence and dichroism, Kishbaugh and McHugh[22] have related structure formation in PS solutions under shear with shear thickening. However, the manner in which anomalous stress, caused specifically by the HF mechanism of fluctuation enhancement, contributes to rheology remains an open question that is addressed in this paper.

The appearance of large anomalous stresses is not limited to poor polymer solutions near a phase boundary but should be present in general for any fluid. The underlying principle for large anomalous stresses appears to be the strength of the coupling between stress, shear, and fluctuations and not necessarily the proximity to a phase boundary. For example, through dynamic light scattering studies, Jian *et al.*[51] have observed a coupling of stress and diffusion in concentrated, entangled poly(butylacrylate) in dioxane, a nominally good solvent. This may then be the mechanism for the high shear rate induced thickening in good solutions observed by Dupuis and co-workers.[48,49] Anomalous stresses may also be present in other kinds of solutions where fluctuations and shear are interactive. Recent scattering studies on wormlike micelle solutions have revealed the appearance of flow-induced butterfly patterns through the HF mechanism,[52−54] while mechanical rheometry has shown the appearance of secondary shear stress overshoots.[54] Other systems where shear-thickening has been observed include telechelic ionomers that undergo physical gelation such as poly(vinyl alcohol) in aqueous borax.[55,56] Further, in similar PVA/borax solutions dynamic and light scattering and dynamic mechanical rheology reveal stress-enhanced concentration fluctuations.[57] Block copolymer micelles also display strong interactions between stress and structure as revealed by small-angle neutron scattering studies on colloidal systems[58] and by stress relaxation measurements on blend systems.[59]

A further unresolved question is how anisotropic concentration fluctuations contribute to the time-dependent stress evolution during flow startup. It is well-known that homogeneous entangled semidilute solutions display a transient overshoot in shear and normal stress when a shear rate is imposed that is sufficiently greater than the inverse longest polymeric relaxation time $\lambda$. This behavior is due to the rapid deformation of polymer chains before their subsequent relaxation. Magda *et al.*[60] and Kume *et al.*[25,26] reported that semidilute solutions of high molecular weight PS in DOP display a second overshoot in stress. Using time-resolved small angle light scattering (SALS), Kume and co-workers have shown that the second overshoot is related to shear-induced demixing. Both the second overshoot and shear thickening become evident when the butterfly pattern characterized by high intensity scattering along the flow direction changes to a streak pattern elongated along the vorticity direction. A second overshoot in the shear stress has also been observed in blends undergoing flow-induced demixing[21] and in micelle solutions undergoing flow-induced structural transitions.[54]

In this paper, we present a model for the anomalous stress that is based on previous models for stress enhancement of concentration fluctuations. Although our analysis is derived through several approximations, features attributed to anomalous stress such as shear thickening and second overshoots in stress are described. The model is phenomenological and therefore experimental verification is of fundamental importance. At the end of the paper, we present results from dichroism experiments on semidilute PS/DOP that show qualitative agreement with predicted time-dependent behavior.

## II. Thermodynamic Stress

The stress tensor due to local fluctuations in concentration fluctuations may be expressed by the so-called anomalous stress first introduced by Sallavanti and Fixman.[35] Derivations of anomalous stress have been developed by a number of authors including Felderhof,[61] Onuki and Kawasaki,[62] Onuki,[41,63] Doi,[64] and Fredrickson and Larson.[39,40] Here, the two-fluid model developed by Brochard and de Gennes[5] and modified by Doi[64] is used as a starting point. Let be $\phi(\mathbf{x})$ the polymer volume fraction. Then the thermodynamic force $\mathbf{F}_p$ on the polymer in a unit volume resulting from concentration fluctuations is given by the functional derivative of the free energy, $F$ [41,63,64]

$$\mathbf{F}_p = -\phi\nabla\left(\frac{\delta F}{\delta \phi}\right) \tag{1}$$

This can be readily shown by relating the rate of change of the free energy to the local polymer velocity $\mathbf{v}_p$.[64] For the free energy functional, the usual coarse-grained Landau−Ginzburg form is used, i.e.

$$F[\phi] = k_B T \int \left(f(\phi) + \frac{K}{2}(\nabla\phi)^2\right) \mathrm{d}\mathbf{x} \tag{2}$$

where $f$ is the dimensionless bulk free energy density and $k_B$ is the Boltzmann constant. The term quadratic in $\nabla\phi$ accounts for the energy cost of concentration inhomogeneities. Then by eq 1,

$$\mathbf{F}_p = -k_B T \phi \nabla(f' - K\nabla^2\phi) \tag{3}$$

The force $\mathbf{F}_p$ can also be written as the divergence of a thermodynamic stress tensor $\Pi$:[41,64,65]

$$\mathbf{F}_p = \nabla\cdot\Pi \tag{4}$$

with

$$\Pi_{ij} = -\pi\delta_{ij} + \sigma^a_{ij} \tag{5}$$

where $\pi \equiv k_B T(\phi f' - f)$ is the osmotic pressure and $\sigma^a$ is the anomalous stress arising from fluctuations:[41,64]

$$\sigma^a = k_B T\{K[^1/_2(\nabla\phi)^2 + \phi\nabla^2\phi]\mathbf{I} - K\nabla\phi\nabla\phi\} \tag{6}$$

If we now consider a homogeneous flow characterized by a velocity gradient $\kappa_{ij} = \partial v_i/\partial x_j$, the equal time correlation function $\langle\delta\phi(\mathbf{x})\delta\phi(\mathbf{x}')\rangle$ is translationally invariant. Here $\delta\phi(\mathbf{x}) \equiv \phi(\mathbf{x}) - \phi_0$ is the local variation from the bulk concentration. The fluctuational stress tensor averaged over possible fluctuational shapes in shear flow can then be expressed as the second moment of the structure factor defined by $S(\mathbf{k}) \equiv \int d\mathbf{x}\, e^{-i\mathbf{k}\cdot(\mathbf{x}-\mathbf{x}')}\langle\delta\phi(\mathbf{x})\delta\phi(\mathbf{x}')\rangle$, i.e.

$$\langle\sigma^a_{ij}\rangle = -p^a\delta_{ij} + \tau^a{}_{ij} \tag{7}$$

where $p^a$ and $\tau^a_{ij}$ are the isotropic and anisotropic contributions defined by

$$\tau^a_{ij} = -k_B TK\int_{\mathbf{k}} k_i k_j S(\mathbf{k}) \tag{8}$$

$$p^a = {}^1/_2 k_B TK\int_{\mathbf{k}} k^2 S(\mathbf{k}) \tag{9}$$

where the short-hand notation $\int_{\mathbf{k}} = (2\pi)^{-3}\int_{k<\Lambda} d\mathbf{k}$ is used and $\Lambda$ is a cutoff wavenumber.

Since the anomalous stress is proportional to the second moment of the structure factor, it corresponds to the degree of anisotropy of the mesostructure. The primary axes of the stress correspond to directions along which fluctuations are preferentially enhanced or suppressed. $\tau^a$ may have profound effects on the rheology and fluid mechanical stability of a system. On the other hand, the osmotic pressure has no direct rheological signature since it is isotropic. In what follows below, we utilize the expression for $\tau^a$ in eq 8 in combination with an evolution equation for the structure factor to formulate a constitutive equation for the anomalous stress. The anomalous stress $\tau^a$ is also related to the stress due to anisotropic droplets in binary mixtures.[66,41] For such a system, Doi and Ohta[67] have developed a constitutive equation for the stress due to anisotropic interface distributions in incompatible blends. Subsequently, Onuki extended the Doi−Ohta model and obtained scaling relations for the growth of anisotropic domains and stress. Their line of argument is similar to that presented below.

## III. Concentration Fluctuation Dynamics

Before developing the evolution equation for the structure factor, we first describe the mechanisms that affect the dynamics of concentration fluctuations. Under flow, essentially three mechanisms affect concentration fluctuations in polymer solutions: (a) local concentration changes as a result of a convective flux driven by the fluid velocity **v**, (b) a diffusive flux driven by the thermodynamic force $\nabla\cdot\Pi$ tends to dissipate fluctuations, and (c) an additional flux resulting from polymer stress gradients $\nabla\cdot\tau^p$ enhances fluctuations. Although the latter HF mechanism has been described in detail elsewhere,[31,32] we shall briefly describe it below since its effect is initially counterintuitive. Consider a polymer concentration fluctuation in simple shear flow. Since rheological coefficients such as the viscosity are concentration dependent, gradients in concentration correspond to gradients in stress. Suppose further that polymers are being stretched along the concentration gradient direction. Hence, regions of high concentration will be under a higher state of stress than adjacent regions of lower concentration. The result is a net force driving polymers from low to high concentration regions. This force is balanced by the drag between solvent and polymer as solvent flows in the opposite direction (from high to low concentration regions). Generally speaking, concentration waves with wave vectors **k** parallel to the extensional axis of the stress $\tau^a$ are enhanced, and waves with **k** perpendicular to the direction of extension are suppressed. Clearly, the relative strengths of the diffusive, convective, and stress-enhancement mechanisms will determine the anisotropy of concentration fluctuations and the structure factor. If diffusion dominates, the system tends to be isotropic. If convection dominates, concentration fluctuations perpendicular to the flow direction are enhanced, and if stress enhancement dominates, concentration fluctuations parallel to the polymeric extensional stress axis are enhanced. Since enhancement of fluctuations along a certain direction corresponds to an increase in the structure factor along that direction, we can use eq 8 to determine three cases for the anomalous stress. (i) Diffusion dominated solutions have small anomalous stresses. (ii) In convection-dominated systems, the principal anomalous stress axis is along the flow direction. (iii) In systems where stress enhancement dominates, the principal anomalous stress axis is perpendicular to the polymeric stress axis.

Three time scales are important. First, the characteristic time scale for the flow field in the case of simple shear flow is the inverse shear rate, $\dot\gamma$. Second, the concentration fluctuations dissipate at a rate $Dk^2$, where $D$ is the cooperative diffusion coefficient. Third, the stress in entangled polymers relaxes according to the reptation time $\lambda$, independent of $k$. Helfand and Fredrickson[7] assumed that the stress fluctuations instantaneously follow concentration fluctuations according to the concentration dependence of the rheological properties. As pointed out by Milner,[31] this assumption is only valid for long-lived, large spatial concentrations and thus small $k$. A wavenumber $k_c$ is defined by the equality of the longest rheological relaxation time and the diffusion time, i.e., $Dk_c^2 = 1/\lambda$.[5,33] Concentration fluctuations with $k > k_c$ relax more quickly than the stress, and in this case, stress and concentration decouple and the stress-enhancement mechanism is no longer effective. The result is a peak near $k_c$ in the stress-enhanced structure factor.

The two-fluid model initially developed by Brochard and de Gennes[5] in the absence of flow describes the coupled dynamics of polymer concentration and stress in a solvent. Doi and Onuki,[9,64] and Milner[10] have extended the two-fluid model to include flow. More recently, Milner[31] and Ji and Helfand[32] have developed generalized canonical models that include coupling with the polymer strain tensor. Here we will briefly present an abbreviated version of the two-fluid model. In formulating a coarse-grained description of fluctuations, fast, microscopic processes are represented by a stochastic term $\theta_\phi$. Hence, the time evolution of polymer volume fraction $\phi(\mathbf{x},t)$ is governed by the Langevin equation,[31]

$$\partial\phi/\partial t + \mathbf{v}\cdot\nabla\phi = -\nabla\cdot[\zeta^{-1}\nabla\cdot(\Pi + \tau^p)] + \theta_\phi \quad (10)$$

where $\zeta^{-1} = \phi\lambda_d^{-1}$ and $\lambda_d$ is the drag coefficient between solvent and polymer generally given by $\lambda_d(\phi) \cong \eta_s\xi_H(\phi)^2$, where $\xi_H$ is the hydrodynamic screening length and $\eta_s$ is the solvent viscosity. In $\theta$ solvents, $\lambda_d \sim \eta_s\phi^2$, and in good solvents, $\lambda_d \sim \eta_s\phi^{2\nu/(3\nu-1)}$.[33]

In the linearized theory, second-order effects in concentration are neglected. Since $\nabla\cdot\Pi = -\phi\nabla(\delta F/\delta\phi)$, eq 10 can be rewritten in the Cahn−Hilliard−Cook[69−72] form with the additional term for the HF mechanism,

$$\frac{\mathrm{D}\phi}{\mathrm{D}t} = \Gamma\nabla^2\frac{\delta F}{\delta\phi} - \Gamma\phi_0^{-1}\nabla\nabla:\tau^p + \theta_\phi \quad (11)$$

where $\mathrm{D}\phi/\mathrm{D}t \equiv \partial\phi/\partial t + \mathbf{v}\cdot\nabla\phi$ is the convected derivative. $\Gamma = \phi_0\zeta^{-1}$ is the mobility, assumed to be constant, and $\phi_0$ is the bulk concentration. The second term on the right-hand side causes fluctuation enhancement by the HF mechanism. For the free energy, the extended Flory−Huggins−de Gennes free energy allowing for slow spatial variations is used:[70]

$$F = k_BT\int\left[\frac{\phi}{N}\ln\phi + (1-\phi)\ln(1-\phi) + \chi\phi(1-\phi) + \frac{a_m^2}{36\phi(1-\phi)}(\nabla\phi)^2\right]\mathrm{d}\mathbf{x} \quad (12)$$

Comparison with eq 2 yields $K = a_m^2/[18\phi(1-\phi)]$, where $a_m$ is a monomer dimension. The bulk free energy density $f(\phi)$ takes a single or double minimum in the one- or two-phase regions, respectively. Typically, $f(\phi) = a\phi^2 + b\phi^4$, where $2a = f_0'' = 1/(1-\phi_0) - 2\chi$ and $f_0''$ is the second derivative of free energy evaluated at the bulk concentration, $\phi_0$. In the one-phase region $a > 0$, while $a < 0$ in the two-phase region. The quartic term $b\phi^4$, with $b > 0$, suppresses runaway growth in the theory of phase separation originating from the Cahn−Hilliard model. In this paper, we will not consider the two-phase region and set $b = 0$. The linearized free energy is then $F = [(k_BT)/2]\int[2a\phi^2 + K(\nabla\phi)^2]\,\mathrm{d}\mathbf{x}$. Then, by the equipartition theorem, the quiescent structure factor $S°(\mathbf{k})$ has the usual Ornstein−Zernicke form,

$$S°(\mathbf{k}) = \frac{k_BT\chi}{1+\xi^2k^2} \quad (13)$$

where $\xi = (K/f_0'')^{1/2}$ is the correlation length and $\chi \equiv (2ak_BT)^{-1}$ is the zero wavelength susceptibility. Further,

$$\frac{\delta F}{\delta\phi} = 2ak_BT(\phi - \xi^2\nabla^2\phi) \quad (14)$$

Insertion of eq 14 into eq 11 gives

$$\frac{\mathrm{D}\delta\phi}{\mathrm{D}t} = D_0\nabla^2(1-\xi^2\nabla^2)\delta\phi - \frac{\Gamma}{\phi_0}\nabla\nabla:\tau^p + \theta_\phi \quad (15)$$

where $D_0 \equiv 2ak_BT\Gamma$ is the "bare" diffusion coefficient. The Gaussian noise correlation satisfies the fluctuation−dissipation theorem,

$$\langle\theta_\phi(\mathbf{x},t)\theta_\phi(\mathbf{x}',t')\rangle = -(2k_BT\Gamma)\nabla^2\delta(\mathbf{x}-\mathbf{x}')\delta(t-t') = -(D_0/a)\nabla^2\delta(\mathbf{x}-\mathbf{x}')\delta(t-t') \quad (16)$$

thus ensuring relaxation to equilibrium at temperature $T$.

In the most recent theories of concentration fluctuations in flowing polymer solutions, coupled Langevin equations are written for fluctuations in concentration, velocity, and the finger strain tensor, $\mathbf{W}$.[31,32] The Langevin equation of motion for the fluid velocity is simply the Navier−Stokes equation with an added random noise variable $\theta_\mathbf{v}$,[7,32]

$$\rho\frac{\mathrm{D}\mathbf{v}}{\mathrm{D}t} = -\nabla p + \eta_s\nabla^2\mathbf{v} + \nabla\cdot\tau^p + \nabla\cdot\Pi + \theta_\mathbf{v} \quad (17)$$

where $\rho$ is the density and $p$ is the pressure. Since the polymer solution is assumed to be incompressible, $\nabla\cdot\mathbf{v} = 0$. The noise $\theta_\mathbf{v}$ satisfies the usual fluctuation−dissipation relation:[73]

$$\langle\theta_\mathbf{v}(\mathbf{x},t)\theta_\mathbf{v}(\mathbf{x}',t')\rangle = -2k_BT\mathbf{I}\nabla\cdot(\eta[\phi(\mathbf{x},t)]\nabla\delta(\mathbf{x}-\mathbf{x}')\delta(t-t')) \quad (18)$$

where $\mathbf{I}$ is the identity tensor and $\eta$ is the overall viscosity of the system. Simplifications can be made since the velocity fluctuations relax much faster than concentration fluctuations, since $\nu/D_0 \gg 1$ (where $\nu = \eta_s/\rho$ is the kinematic viscosity and corresponds to a momentum diffusion coefficient) for typical polymer solutions.[32] As a result, the velocity equation may be eliminated by slaving velocity fluctuations $\delta\mathbf{v}$ to fluctuations in concentration $\delta\phi$ and stress $\delta\tau^p$. Fluctuations in the stress $\delta\tau^p$ appearing in eq 15 are then expressed in terms of concentration and strain through the relationship for rubber elasticity,[74]

$$\tau^p = 2\mathbf{W}\cdot\frac{\delta F_{el}}{\delta\mathbf{W}} \quad (19)$$

where $F_{el}$ is an elastic energy functional. This canonical approach, however, is still problematic since it is only rigorously correct for small velocity gradients. Further, the choice of $F_{el}$ is ambiguous and leads to unsatisfactory constitutive equations for the polymer stress that predict a maximum in the shear stress at moderate shear rates.[32] Instead, we revert to the simplified approach of Helfand and Fredrickson[7] and express the polymeric stress through a convenient differential constitutive equation. Moreover, the purpose of this work is not to develop a more sophisticated theory for the coupled dynamics of concentration fluctuations, but it is rather to describe qualitatively the effect of shear enhanced concentration fluctuations on the rheology of the fluid through the anomalous stress. Although this simplified approach does neglect important effects such as velocity fluctuations and the appearance of the wavenumber $k_c$, we will simply assume its existence and make use of it where appropriate.

## IV. Stress

The total stress $\tau$ is assumed to be the sum of a solvent contribution $\tau^s$, a polymer contribution $\tau^p$, and an anomalous contribution $\tau^a$,

$$\tau = \tau^s + \tau^p + \tau^a \quad (20)$$

The solvent contribution is assumed to be Newtonian, $\tau^s = 2\eta_s\mathbf{D}$, where $D_{ij} \equiv {}^1/_2(\kappa_{ij} + \kappa_{ji})$ is the rate of strain tensor.

For the polymeric contribution, the Giesekus equation is used:[74]

$$\tau^p + \lambda\check{\tau}^p + \frac{\alpha_G}{G}\tau^p\cdot\tau^p = 2\eta_p\mathbf{D} \tag{21}$$

where $G$ is the plateau modulus, $\eta_p$ is the polymer viscosity, and the upper convected time derivative is defined as $\check{\tau}_{ij} = (\partial\tau^p_{ij}/\partial t) - (\kappa_{ik}\tau^p{}_{kj} + \tau^p{}_{ik}\kappa_{jk})$. The quadratic term in $\tau^p$ in eq 21corresponds to an anisotropic drag term for stretched polymers and typically $\alpha_G = 0.6$. The Giesekus equation was chosen since it is simple yet qualitatively accurate for simple shear flows at low and moderate shear rates: it predicts overshoots in the shear stress $\tau^p_{xy}$ and the first normal stress difference $N_1 = \tau^p_{xx} - \tau^p_{yy}$ on flow inception, shear thinning, and a correct ratio of the second normal stress difference $N_2 = \tau^p_{yy} - \tau^p_{zz}$ to the first normal stress difference ($-N_2/N_1 = 0.3$) in the zero-shear limit.[75] Stress-induced fluctuation enhancement results from the concentration dependence of the relaxation time $\lambda$ and the plateau modulus $G = \eta_p/\lambda$. For semidilute entangled polymer solutions:[76]

$$\lambda \sim \phi^{3/2}; \quad G \sim \phi^{9/4} \tag{22}$$

The polymer stress fluctuation $\delta\tau^p = \tau^p - \tau^{p\circ}$ is then slaved to $\delta\phi$ through eq 21 as follows:

$$\delta\tau^p + \lambda\left(\frac{\beta_p}{\phi_0}\check{\tau}^p\delta\phi + \delta\check{\tau}^p\right) + \frac{\alpha_G}{G}\left(\tau^p\cdot\delta\tau^p + \delta\tau^p\cdot\tau^p - \frac{\alpha_p}{\phi_0}\tau^p\cdot\tau^p\delta\phi\right) = 2\frac{\eta_p}{\phi_0}(\alpha_p + \beta_p)\mathbf{D}\delta\phi \tag{23}$$

where $\alpha_p$ and $\beta_p$ denote the scaling exponents of the plateau modulus and the relaxation time with respect to concentration, respectively. If these are not of order unity, large shear rates are required before shear enhancement becomes important. By eq 22,

$$\alpha_p = \frac{\partial}{\partial \ln \phi}\ln G = \frac{9}{4}, \quad \beta_p = \frac{\partial}{\partial \ln \phi}\ln \lambda = \frac{3}{2}$$

If the appropriate scaling for $\theta$ solutions ($\lambda \sim \phi^3$) is used, there is no effect on the linearized model developed in this paper other than multiplying $\alpha_p$ by a factor of 2. In what follows, we will make the substitution

$$\tau'\delta\phi = \phi_0\delta\tau^p \tag{24}$$

## V. Dimensionless Equations

It is convenient to write the governing equations in dimensionless form. For this purpose, we choose $k_c^{-1}$ as the characteristic length. To choose the characteristic time scale, we use the diffusive time scale, $\tau_D \equiv 1/(D_0k_c^2)$. For the characteristic velocity, we use the convective scale $k_c^{-1}\dot{\gamma}$ The characteristic stress scale presents several choices: for the polymeric stress, we choose the elastic modulus $G \equiv \eta_p/\lambda$; for the anomalous stress, we choose the inverse susceptibility, $\chi^{-1} \equiv 2ak_BT$, associated with osmotic pressure. The dimensionless variables,

$$\tilde{t} = t/\tau_D; \quad \tilde{\mathbf{v}} = (k_c/\dot{\gamma})\mathbf{v}; \quad \tilde{\nabla} = k_c^{-1}\nabla; \quad \tilde{\tau}^p = \tau^p/G; \quad \tilde{\tau}^a = \chi\tau^a; \quad \tilde{\theta}_\phi = t_D\theta_\phi$$

are then substituted into the governing equations. Equation 15 then becomes

$$\frac{\partial\delta\phi}{\partial t} + Pe\tilde{\mathbf{v}}\cdot\tilde{\nabla}\delta\phi = \tilde{\nabla}^2(\delta\phi - x^2\tilde{\nabla}^2\delta\phi) - \frac{1}{\Xi}\tilde{\nabla}\tilde{\nabla}:\tilde{\tau}'\delta\phi + \tilde{\theta}_\phi \tag{25}$$

where $x \equiv \xi k_c$ is the dimensionless correlation length. The Peclet number $Pe \equiv \dot{\gamma}\tau_D = \dot{\gamma}/(D_0k_c^2)$ represents the strength of coupling between convection and diffusion. Recalling that $D_0 \equiv \chi^{-1}\Gamma$, the coupling parameter between stress and concentration fluctuations is

$$\frac{1}{\Xi} \equiv \frac{\tau_D k_c^2\Gamma G}{\phi_0^2} = G\phi_0^{-2}\chi \tag{26}$$

which is a measure of the relative ease of dilating the transient gel and diluting the solution. If the solution is not easily compressed as in a good solvent, $\Xi^{-1} \ll 1$ and concentration is decoupled from stress. In this case, the conventional Cahn−Hilliard−Cook form of the Langevin equation is recovered. In $\theta$ and poor solvents, osmotic forces become relatively weak, $\Xi \sim 1$, and the effect of the coupling becomes significant. This effect can also dramatically slow down the growth of nucleating droplets in the metastable states.[9]

Using our normalized variables, eq 16 is written in dimensionless form

$$\langle\tilde{\theta}_\phi(\tilde{\mathbf{r}},\tilde{t})\tilde{\theta}_\phi(\tilde{\mathbf{r}}',\tilde{t}')\rangle = -\left(\frac{1}{\alpha}\right)\tilde{\nabla}^2\tilde{\delta}(\tilde{\mathbf{r}} - \tilde{\mathbf{r}}')\delta(\tilde{t} - \tilde{t}') \tag{27}$$

where the parameter $\alpha = ak_c^{-3}$ affects the strength of the noise in the evolution equation.

The dimensionless constitutive equation for the polymeric stress is written as

$$\tilde{\tau}^p + De\check{\tilde{\tau}}^p + \alpha_G\tilde{\tau}^p\cdot\tilde{\tau}^p = 2De\tilde{\mathbf{D}} \tag{28}$$

and

$$\tilde{\tau}' + De(\beta_p\check{\tilde{\tau}}^p + \check{\tilde{\tau}}') + \alpha_G(\tilde{\tau}^p\cdot\tilde{\tau}' + \tilde{\tau}'\cdot\tilde{\tau}^p - \alpha_p\tilde{\tau}^p\cdot\tilde{\tau}^p) = 2De(\alpha_p + \beta_p)\tilde{\mathbf{D}} \tag{29}$$

where $De \equiv \lambda\dot{\gamma}$ is the Deborah number and the dimensionless upper convected time derivative is defined as

$$\check{\tilde{\tau}}_{ij} = \frac{1}{Pe}\frac{\partial\tilde{\tau}^p_{ij}}{\partial\tilde{t}} - (\tilde{\kappa}_{ik}\tilde{\tau}^p{}_{kj} + \tilde{\tau}^p{}_{ik}\tilde{\kappa}_{jk}) \tag{30}$$

Further, an isotropic term $\alpha_p\delta_{ij}$ corresponding to the concentration dependence of the modulus is added to $\tilde{\tau}_{ij}'$.

The dimensionless anomalous stress expression is obtained from eq 8, $\tau^a_{ij} = -\xi^2/\chi\int_{\mathbf{k}}k_ik_jS(\mathbf{k})$. Hence,

$$\tilde{\tau}^a_{ij} = -x^2\int_{\mathbf{k}}\tilde{k}_i\tilde{k}_j\tilde{S}(\tilde{\mathbf{k}}) \tag{31}$$

where $\tilde{S} = Sk_c^3$ is the normalized structure factor.

In what follows, the " ˜ " symbol to denote dimensionless variables is dropped. So far, the model is based on eqs 25, 27−29, and 31. The dimensionless model parameters are $\Xi = \phi_0^2\chi^{-1}/G$, $De = \lambda\dot{\gamma}$, $\alpha = ak_c^{-3}$, $x = \xi k_c$, and $Pe = \tau_D\dot{\gamma}$. The model parameters may all be measured by light scattering and rheology. Using dynamic viscosity measurements, the plateau modulus and stress relaxation time together with their concentration dependence may be obtained. The diffusion coefficient can be determined from dynamic light scattering or time-resolved small angle light scattering

(SALS) after flow cessation, while taking into account stress−diffusion coupling[14] while the osmotic compressibility $\chi^{-1}$ can be measured by absolute intensity static light scattering or osmometry. $\xi$ can be obtained by static light scattering and $k_c$ can be calculated from the diffusion coefficient and the stress relaxation time or can be measured directly from the peak position in SALS patterns during flow.[54]

## VI. Constitutive Model for the Anomalous Stress

In this section, we outline the procedure for obtaining a constitutive model for the anomalous stress. First, the dimensionless, linearized evolution equation for concentration fluctuations (eq 25) is expressed in Fourier space,

$$\frac{\partial \phi_{\mathbf{k}}}{\partial t} = Pe\,\mathbf{k}\cdot\kappa\cdot\frac{\partial \phi_{\mathbf{k}}}{\partial \mathbf{k}} - k^2(1 + x^2k^2)\phi_{\mathbf{k}} + \frac{1}{\Xi}\mathbf{kk}:\tau'\phi_{\mathbf{k}} + \theta_{\mathbf{k}} \tag{32}$$

where $\phi_{\mathbf{k}} = \int e^{i\mathbf{k}\cdot\mathbf{x}}\delta\phi(\mathbf{x})\,d\mathbf{x}$ and $\mathbf{k}$ is the wave vector made dimensionless with respect to $k_c$. By eq 27, the Gaussian noise $\theta_{\mathbf{k}}$ in Fourier space is $\delta$ correlated as follows,

$$\langle\theta_{\mathbf{k}}\theta_{\mathbf{k}'}\rangle = \frac{k^2}{\alpha}\delta_{\mathbf{k}+\mathbf{k}'} \tag{33}$$

By multiplying each term in eq 32 by $\phi_{-\mathbf{k}}$ and averaging, an evolution equation is obtained for the structure factor,

$$\frac{\partial S}{\partial t} = Pe\,\mathbf{k}\cdot\kappa\cdot\frac{\partial S}{\partial \mathbf{k}} - 2k^2(1 + x^2k^2)S + \frac{2}{\Xi}\mathbf{kk}:\tau'S + \frac{k^2}{\alpha} \tag{34}$$

where we have used the equality $\langle\theta_{\mathbf{k}}(t)\,\phi_{-\mathbf{k}}(t)\rangle + \langle\theta_{-\mathbf{k}}(t)\,\phi_{\mathbf{k}}(t)\rangle = k^2/\alpha$.[76] From eq 13, the quiescent structure factor made dimensionless with respect to the volume $k_c^{-3}$ is

$$S^\circ(\mathbf{k}) = \frac{1}{2\alpha}\frac{1}{1 + x^2k^2} \tag{35}$$

consistent with eq 34. The evolution equation for the structure factor including the effect of stress coupling was first derived by Helfand and Fredrickson.[7] At steady state, when $Pe \ll 1$ (i.e., no convection) and $k < k_c$, $S(\mathbf{k})$ takes the general anisotropic form:

$$S(\mathbf{k}) = \frac{1}{2\alpha}\frac{1}{1 + k^2 - a_0k^2 - a_1k_xk_y - a_2(k_x^2 - k_y^2) - a_3(k_y^2 - k_z^2)} \tag{36}$$

where the coefficients $a_i$ originate from fluctuations in components of the polymer stress tensor and depend on rheological parameters and the applied strain rate. For example, in simple shear flow ($v_x = \dot{\gamma}y$), the structure factor in the $x-y$ plane is a so-called butterfly pattern,[12,13] with high intensity lobes oriented along an axis at an angle $\chi'$ that varies from 45° to 0° to the flow direction (the $x$ axis). As expected, $\chi'$ follows the same trends as the orientation of the principal stress axis as measured by intrinsic birefringence.[13] Considering eq 31, the corresponding anomalous stress for such a butterfly pattern is characterized by a negative shear stress $\tau_{xy}^a$ and a negative first normal stress difference $N_1^a$. The structure factor can be calculated more accurately up to $De \cong 1$ by using the method of characteristics to solve the full set of coupled canonical equations that include strain and velocity fluctuations in addition to eq 34.[31,32] The object of these studies was not to determine the anomalous stress but rather to accurately calculate structure factors.

In this work we follow a different approach. An equation of motion for the second moment of the structure factor is developed and thus a constitutive equation for the anomalous stress is obtained. We multiply the evolution equation for the structure factor by the dyad $\mathbf{kk}$ and integrate over $k < \Lambda$:

$$\frac{-1}{x^2}\frac{\partial \tau^a}{\partial t} = Pe\int_{\mathbf{k}}\mathbf{kkk}\cdot\kappa\cdot\frac{\partial S}{\partial \mathbf{k}} - 2\int_{\mathbf{k}}\mathbf{kk}k^2(1 + x^2k^2)S + \frac{2}{\Xi}\int_{\mathbf{k}}\mathbf{kkkk}:\tau'S + \int_{\mathbf{k}}\mathbf{kk}\frac{k^2}{\alpha} \tag{37}$$

As explained above, the stress enhancement of concentration fluctuations begins to break down at wavenumbers greater than $k_c$, thus giving rise to a peak in $S(\mathbf{k})$ at dimensional wavenumber $k \cong k_c$. Therefore, stress-induced anisotropy in $S(\mathbf{k})$ and $\tau^a$ occurs only up to wavenumbers around $k_c$. In the analysis that follows, a dimensionless cutoff wavenumber $\Lambda = 2$ is chosen. Although this choice is somewhat arbitrary, to capture the anisotropy in $S(\mathbf{k})$, one should choose $\Lambda > 1$ and $\Lambda \sim O(1)$. This holds true for both poor and good solutions. This then introduces two regimes: (i) $\Lambda x > 1$ and (ii) $\Lambda x < 1$. In case (i) quiescent concentration fluctuations strongly couple to stress because $\xi^2/D > \lambda$. In case (ii) quiescent concentration fluctuations with correlation length $\xi$ do not couple to stress because $\xi^2/D < \lambda$. The concentration gradient term in the free energy is unimportant to the anomalous stress and the dynamics of $\tau^a$ become independent of $x$. In order to solve eq 37, the following quiescent initial conditions are obtained by integrating $S^\circ(k)$:

$$\tau_{kk}^{a\,\circ} \cong \frac{-2\pi}{\alpha x^3}\frac{(\Lambda x)^5}{5}, \quad Q^\circ \cong \frac{2\pi}{\alpha x^3}\frac{(\Lambda x)^3}{3}; \quad \Lambda x < 1 \tag{38}$$

$$\tau_{kk}^{a\,\circ} \cong \frac{-2\pi}{\alpha x^3}\frac{(\Lambda x)^3}{3}, \quad Q^\circ \cong \frac{2\pi}{\alpha x^3}\Lambda x; \quad \Lambda x > 1 \tag{39}$$

where $Q^\circ = \int_{\mathbf{k}}S^\circ(k)$.

We shall now express each term in eq 37 in terms of $\tau^a$. Integrating the convective term, we obtain

$$\int_{\mathbf{k}}k_ik_jk_k\kappa_{kl}\frac{\partial}{\partial k_l}S(\mathbf{k}) = -\int_{\mathbf{k}}(\kappa_{ki}k_kk_j + k_ik_k\kappa_{kj})\,S(\mathbf{k}) = \frac{1}{x^2}(\kappa_{ki}\tau_{kj}^a + \tau_{ik}^a\kappa_{kj}) \tag{40}$$

Here, we have assumed that on applying the divergence theorem, the surface integral on the surface $S_\Lambda$ at $k = \Lambda$ is zero as $S(\Lambda) \cong 0$. This assumption is correct if $\Lambda x \gg 1$. If, however, $\Lambda x < 1$, then on the surface $S_\Lambda$, $S(k) \cong 1/2\alpha$ and the surface integral in eq 40 is nonzero and is given by

$$\int_{\mathbf{k}} \frac{\partial}{\partial k_l}[k_i k_j k_k \kappa_{kl} S(\mathbf{k})] = \Lambda^3 S^\circ(\Lambda)\, \kappa_{kl} \int_{S_\Lambda} l_i l_j l_k l_l =$$

$$\frac{4\pi\Lambda^5}{15} S^\circ(\Lambda)\kappa_{kl}(\delta_{ik}\delta_{jl} + \delta_{il}\delta_{jk}) = \kappa_{ki}\tau^{a}_{kj}{}^\circ + \tau^{a}_{ik}{}^\circ \kappa_{kj} \quad (41)$$

where $\mathbf{l} = \mathbf{k}/k$ is the outward unit normal vector on $S_\Lambda$.

The third term on the right-hand side of eq 37 contains the fourth moment $\overline{\mathbf{kkkk}}:\tau'$ (where $\bar{A} \equiv \int_{\mathbf{k}} A(\mathbf{k})S(\mathbf{k})$ represents an average over the structure factor). To obtain a closed equation for the second moment $\overline{\mathbf{kk}}$ and thus for the anomalous stress, a decoupling approximation similar to that employed by Doi and Ohta[67] is utilized. Consequently, we impose

$$\overline{k_i k_j k_k k_l}\tau'_{kl} = c(\overline{k_i k_j}\cdot\overline{k_k k_l} + \overline{k_i k_k}\cdot\overline{k_j k_l} + \overline{k_i k_l}\cdot\overline{k_j k_k})\tau'_{kl} \quad (42)$$

$c$ is a constant chosen so that eq 42 is rigorously correct when the structure factor has the isotropic, Ornstein−Zernicke form

$$S \sim (1 + \epsilon^2 k^2)^{-1} \quad (43)$$

For now, the dimensionless length $\epsilon$ is assumed to be such that $\Lambda\epsilon \gg 1$. Hence,

$$\overline{k_i k_j k_k k_l} = \frac{4\pi A\Lambda^5}{75\epsilon^2}(\delta_{ij}\delta_{kl} + \delta_{ik}\delta_{jl} + \delta_{il}\delta_{jk}) \quad (44)$$

and

$$\overline{k_i k_j}\cdot\overline{k_k k_l} + \overline{k_i k_k}\cdot\overline{k_j k_l} + \overline{k_i k_l}\cdot\overline{k_j k_k} = \frac{16\pi^2 A^2\Lambda^6}{81\epsilon^4}(\delta_{ij}\delta_{kl} + \delta_{ik}\delta_{jl} + \delta_{il}\delta_{jk}) \quad (45)$$

Hence,

$$c = \frac{27}{25}\frac{1}{Q} \quad (46)$$

where $Q \equiv \bar{1} = \int_{\mathbf{k}} S(k)$ represents the fluctuational energy for $k < \Lambda$ per unit volume. Making use of the symmetry of $\tau'_{kl}$ and combining eqs 44 and 45 result in the decoupling approximation

$$\overline{k_i k_j k_k k_l}\tau'_{kl} = \frac{27}{25x^4 Q}(\tau^a{}_{ij}\tau^a{}_{kl} + 2\tau^a{}_{ik}\tau^a{}_{jl})\tau'_{kl} \quad (47)$$

The second term in eq 37 corresponds to the relaxation of concentration fluctuations through diffusion. To obtain a closed relation for the second moment, $\overline{\mathbf{kk}}$, we impose

$$\overline{k_i k_j k^2(1 + x^2 k^2)} = d_1(\overline{k_i k_j})\cdot\overline{k^2}\cdot(1 + d_2 x^2\overline{k^2}) \quad (48)$$

where $d_1$ and $d_2$ are constants, again chosen so that eq 48 is rigorously correct when the structure factor has the isotropic form in (43). In the limit, $\Lambda\epsilon \gg 1$,

$$\overline{k_i k_j k^2(1 + x^2 k^2)} = \frac{4\pi A}{\epsilon^2}\left(\frac{\Lambda^5}{5} + \frac{x^2\Lambda^7}{7}\right)\frac{\delta_{ij}}{3} \quad (49)$$

and

$$d_1(\overline{k_i k_j})\cdot\overline{k^2}\cdot(1 + d_2 x^2\overline{k^2}) = d_1\left(\frac{4\pi A\Lambda^3}{3\epsilon^2}\right)^2\left[1 + d_2 x^2\left(\frac{4\pi A\Lambda^3}{3\epsilon^2}\right)\right]\frac{\delta_{ij}}{3} \quad (50)$$

Hence

$$d_1 = \frac{9}{5Q} \quad \text{and} \quad d_2 = \frac{15}{7Q} \quad (51)$$

Thus the decoupling approximation is

$$\overline{k_i k_j k^2(1 + x^2 k^2)} = \frac{1}{x^2}\tau^a_{ij} g(\tau^a, Q) \quad (52)$$

where

$$g(\tau^a, Q) \equiv \frac{9}{5}\frac{\tau^a_{kk}}{Qx^2}\left(1 - \frac{15}{7}\frac{\tau^a_{ll}}{Q}\right) \quad (53)$$

Since the noise term integral in eq 37 is always isotropic, it is proportional to the Kronecker delta, $\delta_{ij}$. We utilize the same decoupling approximation as for the diffusion term above, i.e.,

$$\frac{1}{\alpha}\int_{\mathbf{k}} k_i k_j k^2 = 2\frac{\tau^{a\circ}_{ij}}{x^2} g(\tau^a{}^\circ, Q^\circ) \quad (54)$$

By eqs 40, 47, 52, and 54, we can rewrite eq 37 as

$$\frac{\partial\tau^a_{ij}}{\partial t} + Pe(\kappa_{ki}\tau^a_{kj} + \tau^a_{ik}\kappa_{kj}) = 2\Delta(\tau^a_{ij} g) - \frac{2.16}{\Xi Q x^2}(\tau^a_{ij}\tau^a_{kl} + 2\tau^a_{ik}\tau^a_{jl})\tau'_{kl}, \quad \Lambda x > 1 \quad (55)$$

where $\Delta(\tau^a_{ij} g) \equiv \tau^a_{ij} g(\tau^a, Q) - \tau^{a\circ}_{ij} g(\tau^a{}^\circ, Q^\circ)$ represents the relaxation of anisotropy through diffusion. Notice that the integration by parts of the convective term (eq 40) leads to the covariant time derivative for the stress $\tau^a$. The terms on the left-hand side of eq 55 comprise a lower convected derivative $\hat{\tau}^a_{ij}$ defined by

$$\hat{\tau}^a_{ij} \equiv \frac{\partial\tau^a_{ij}}{\partial t} + Pe(\kappa_{ki}\tau^a_{kj} + \tau^a_{ik}\kappa_{kj}) \quad (56)$$

and is a sufficient form of the time derivative to preserve frame invariance.[74,77]

When $\Lambda x < 1$, the surface integral from eq 41 is included and we obtain

$$\frac{\partial\tau^a_{ij}}{\partial t} + Pe(\kappa_{ki}\Delta\tau^a_{kj} + \Delta\tau^a_{ik}\kappa_{kj}) = 2\Delta(\tau^a_{ij} g) - \frac{2.16}{\Xi Q x^2}(\tau^a_{ij}\tau^a_{kl} + 2\tau^a_{ik}\tau^a_{jl})\tau'_{kl} \quad (57)$$

where $\Delta\tau^a_{ij} = \tau^a_{ij} - \tau^{a\circ}_{ij}$.

In order to solve eq 55, an evolution equation for the fluctuational energy $Q$ is required. By integration of eq 34 over $k < \Lambda$,

$$\frac{\mathrm{d}Q}{\mathrm{d}t} = -2\int_{\mathbf{k}} k^2(1 + x^2 k^2)S + \frac{2}{\Xi}\int_{\mathbf{k}} \mathbf{kk}:\tau' S + \frac{1}{\alpha}\int_{\mathbf{k}} k^2 \quad (58)$$

Note that convection has no effect on the overall

fluctuational energy as the system is translationally invariant. As before, we use decoupling approximations to relate the above terms to $\tau^a$, i.e.,

$$\int_{\mathbf{k}} k^2(1 + x^2k^2)S = -\frac{\tau^a_{kk}}{x^2}\left(1 - \frac{9}{5}\frac{\tau^a_{kk}}{Q}\right) = -\frac{\tau^a_{kk}}{x^2}f(\tau^a, Q) \tag{59}$$

Equation 58 then becomes

$$\frac{\mathrm{d}Q}{\mathrm{d}t} = \frac{2}{x^2}\Delta(\tau^a_{kk}f) - \frac{2}{\Xi x^2}\tau^a_{kl}\tau'_{kl} \tag{60}$$

where $\Delta(\tau^a_{kk}f) \equiv \tau^a_{kk}f(\tau^a, Q) - \tau^a_{kk}{}^\circ f(\tau^{a\circ}, Q^\circ)$. The coupled equations 55 and 56 can now be solved to obtain the time-dependent anomalous stress $\tau^a$ and integrated scattering intensity, $Q$. In deriving the coefficients in the above decoupling approximations, the arbitrary length scale $\epsilon$ with $\Lambda\epsilon \gg 1$ was introduced. If instead the limit $\Lambda\epsilon \ll 1$ is used, the following values are obtained for the decoupling coefficients: $c = 5/(7Q)$, $d_1 = 25/(21Q)$, $d_2 = 35/(27Q)$, and $d_3 = 25/(21Q)$. The choice of $\epsilon$ does not seem to have a significant effect.

## VII. Stress-Optic Rule

In this section, we develop a new stress−optic rule to allow measurement of the anomalous stress using birefringence or dichroism. The refractive index tensor $n_{\alpha\beta}$ is in general complex, $n_{\alpha\beta} = n_{\alpha\beta}' + in_{\alpha\beta}''$, where the first and second terms are the real and imaginary parts, respectively. In general, both $n_{\alpha\beta}'$ and $n_{\alpha\beta}''$ contain an intrinsic contribution due to molecular orientation and a form or scattering contribution. The polymeric stress tensor $\tau^p_{\alpha\beta}$ can be shown to be directly proportional to $n_{\alpha\beta}'$ [76] and so is often measured by using intrinsic birefringence and the stress−optic rule.[78] Since mechanical rheometry does not differentiate types of stress, it would be useful if the anomalous stress could also be detected by using a rheo-optical technique. Dichroism is the difference between the eigenvalues of $n_{\alpha\beta}''$ and in the visible spectrum typically arises from form effects due to scattering of light from anisotropic concentration fluctuations. It is related to the second moment of the structure factor $S(\mathbf{k})$ as determined by the Onuki and Doi relation for light scattering from concentration fluctuations,[79]

$$n^f_{\alpha\beta}{}'' = \frac{{k_0}^3}{8\pi^2 n}\left(\frac{\partial n}{\partial \phi}\right)^2 \int \mathrm{d}\Omega_{\hat{\mathbf{k}}_s}(\delta_{\alpha\beta} - \hat{k}_{s_\alpha}\hat{k}_{s_\beta})S(\mathbf{k}) \tag{61}$$

where $\int \mathrm{d}\Omega_{\hat{k}_s}$ denotes integration over the solid angle of the unit propagation vector $\hat{\mathbf{k}}_s$ of scattered light. $n$ is the bulk refractive index and $k_0$ is the wavenumber of the incident light. The Onuki−Doi relation has been verified experimentally by comparing dichroism measured by polarimetry with that calculated from the anisotropy of small angle light scattering patterns.[13,14] The angle of dichroism $\chi''$ is usually defined as the angle of the principal axis of $n''_{\alpha\beta}$ relative to the $x$ axis and is perpendicular to the preferential orientation of concentration gradients and parallel to the principal axis of $\tau^a_{\alpha\beta}$. The shear component and first normal difference of $n_{\alpha\beta}''$ are defined respectively as

$$n_{xy}'' = \frac{\Delta n''}{2}\sin 2\chi'' \quad \text{and} \quad N_1'' = \Delta n''\cos 2\chi'' \tag{62}$$

Consider a small-angle light scattering experiment where $\mathbf{k}_i$ and $\mathbf{k}_s$ are the propagation vectors of incident and scattered light, respectively. Let $\theta$ be the scattering angle and let $\phi$ be the azimuthal angle in the plane perpendicular to $\mathbf{k}_i$. The scattering wavenumber is then $k = 2k_0 \sin(\theta/2)$ since $\mathbf{k} = \mathbf{k}_s - \mathbf{k}_i$. For small $\theta$, $k \cong k_0\theta$ and the integral over $\Omega_{\hat{k}_s}$ in eq 61 can be expressed in terms of an integral over the scattering vector $\mathbf{k}$ as follows

$$\int_0^\pi \mathrm{d}\theta \sin\theta \int_0^{2\pi} \mathrm{d}\phi(\delta_{\alpha\beta} - \hat{k}_{s_\alpha}\hat{k}_{s_\beta})S(\mathbf{k}) \cong \frac{1}{k_0^4}\int_0^{k_m}\int_0^{2\pi} k\,\mathrm{d}k\,\mathrm{d}\phi({k_0}^2\delta_{\alpha\beta} - k_\alpha k_\beta)S(\mathbf{k}) \tag{63}$$

where $k_m$ is the wavenumber at the maximum angle of scattering. Hence, except for an isotropic part,

$$n^f_{\alpha\beta}{}'' \sim -\int \mathrm{d}\mathbf{k} k_\alpha k_\beta S(\mathbf{k}) \tag{64}$$

Considering eq 8, it is tempting to deduce that $n_{\alpha\beta}''$ is proportional to the anomalous stress $\tau^a_{\alpha\beta}$ when $k_c < k_m$ (i.e., when the anisotropy in $S(\mathbf{k})$ occurs predominantly at small scattering angles). Unfortunately, the domain of the integration in eq 64 is the two-dimensional plane perpendicular to $\mathbf{k}_i$, while that in eq 8 is over three-dimensional $k$-space. Hence, there is no rigorous stress−optic rule between dichroism and anomalous stress as there is between intrinsic birefringence $n^i_{\alpha\beta}{}'$ and polymeric stress $\tau^p_{\alpha\beta}$. However, under most conditions, we can still expect that $n_{xy}''$ and $N_1''$ are roughly proportional to $\tau^a_{xy}$ and $N^a_1$, respectively. In the sections below, the significance of dichroism will be very useful in comparing experimental results with model predictions.

As with form dichroism, form birefringence can also be expressed in terms of a second moment of the structure factor by the theory of Onuki and Doi.[79] If the anisotropy in $S(\mathbf{k})$ is not too great, then $S(\mathbf{k})$ can be written as

$$S(\mathbf{k}) \cong S^{(0)}(k) + k_\mu k_\nu S^{(1)}_{\mu\nu}(k) \tag{65}$$

where $S^{(0)}(k)$ and $S^{(1)}_{\mu\nu}(k)$ are independent of $\hat{\mathbf{k}}$. Then in the limit $k \ll 2k_0$,[79]

$$n^f_{\alpha\beta}{}' = \frac{-1}{6\pi^2 k_0^2 n}\left(\frac{\partial n}{\partial \phi}\right)^2 \int_0^\infty \mathrm{d}k k^6 S^{(1)}_{\alpha\beta}(k) \tag{66}$$

From the expansion in eq 65, the anomalous stress (in dimensional units) is

$$\tau^a_{\alpha\beta} = -\frac{8\pi\xi^2\chi^{-1}}{15}\int_0^\infty \mathrm{d}k k^6 S^{(1)}_{\alpha\beta}(k) \tag{67}$$

In deriving the above relations, the terms proportional to $\delta_{\alpha\beta}$ and $k_\alpha k_\beta$ were not written explicitly, because they do not contribute to the birefringence. Comparison of eq 66 with eq 67 leads to a "second" stress−optic rule relating form birefringence to anomalous stress, i.e.,

$$\tau^a_{\alpha\beta} - \frac{1}{3}\delta_{\alpha\beta}\tau^a_{\nu\nu} = \frac{1}{C_{II}}\left(n^f_{\alpha\beta}{}' - \frac{1}{3}\delta_{\alpha\beta}n^f_{\nu\nu}{}'\right) \tag{68}$$

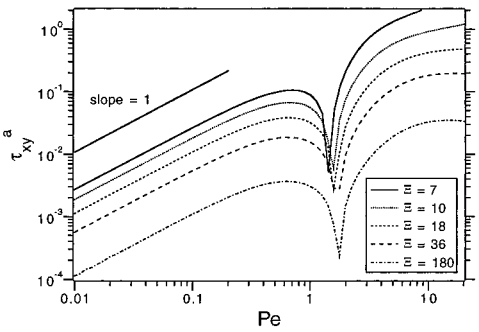


**Figure 1.** Steady-state absolute shear anomalous stress, $\tau^a_{xy}$, as a function of *Pe*, for a range of Ξ. At low shear rates (*Pe* < 2), $\tau^a_{xy}$ is negative.

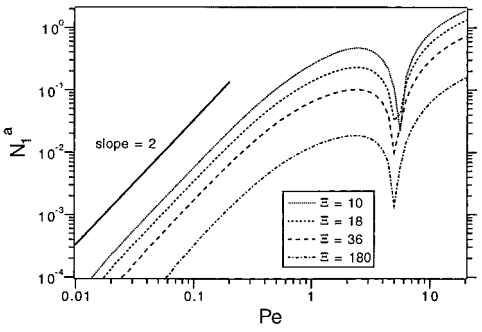


**Figure 2.** Steady-state absolute first normal anomalous stress difference, $N^a_1$, as a function of *Pe*, for a range of Ξ. At shear rates such that *Pe* < 6, $N^a_1$ is negative.

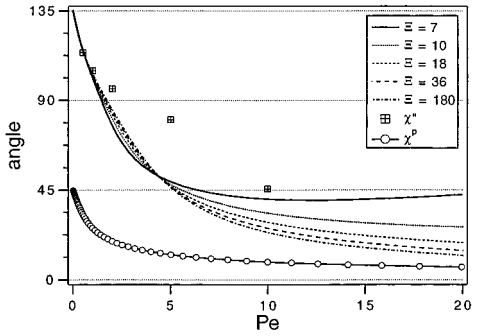


**Figure 3.** Steady-state anomalous stress angle, $\chi^a$, and polymer stress angle, $\chi^p$ as a function of *Pe*, for various values of Ξ. When $\chi^a$ < 90° the anomalous stress causes a relative shear thickening.

where

$$C_{II} \equiv \frac{16\pi^3\chi^{-1}k_0^2\xi^2}{\frac{5}{n}\left(\frac{\partial n}{\partial \phi}\right)^2} \tag{69}$$

is the "second" stress−optic coefficient. The limitation of the above relations is that anisotropic scattering that contributes to the form birefringence must be at small angles. This means that the peak wavenumber in the structure factor, $k_c$, must be much less than the wavenumber $k_0$ of the probing beam. Note that in deriving eq 66, the domain of integration is over three-dimensional *k*-space (see ref 79 for details). It would thus appear that birefringence would be a more appropriate optical probe of anomalous stress than dichroism. However, the linear approximation of eq 65 limits the generality of eq 68 since it is expected that higher-order nonlinear terms are important at high shear rates. Moreover, for most polymer solutions intrinsic birefringence is much stronger than form birefringence, although this is not the case in block copolymer near the ordering transition.[40]

## VIII. Results and Discussion

In this section, steady-state and time-dependent predictions of the constitutive relation are presented. Although there are no adjustable parameters in the model, there are a number of approximations that introduce errors. However, the qualitative trends and time-dependent features of the model will be shown to be in agreement with experimental results. The numerical results presented are for eq 57 with values of the dimensionless parameters, $x = 0.1$, $\Lambda = 2$, equal polymeric and diffusional characteristic times $\tau_D = \lambda = 1.0$, and a range of shear rates and values for the coupling parameter Ξ. Values chosen for the constants introduced during the decoupling approximations correspond to the limit $\Lambda\epsilon \ll 1$.

**VIIIA. Steady-State Predictions.** Consider a viscoelastic fluid in simple shear flow, with the velocity in the *x* direction and the velocity gradient in the *y* direction, i.e., $v_x = \dot{\gamma}y$. We investigate the effect of shear rate on the response of the anomalous stress components. The shear component $\tau^a_{xy}$ and the normal stress difference $N^a_1 = \tau^a_{xx} - \tau^a_{yy}$ as a function of shear rate for a range of Ξ values are presented in Figures 1 and 2, respectively. $\tau^a_{xy}$ and $N^a_1$ are negative for *Pe* < 2 and *Pe* < 6, respectively. Since logarithmic scaling is used in the figures, only absolute values are shown. At low shear rates (*Pe* < 1), $\tau^a_{xy}$ and $N^a_1$ become increasingly negative, indicating that the anisotropic structure factor is oriented preferentially along the principle polymer stress axis and that the stress-enhancement (HF) mechanism contribution to the anomalous stress dominates. At very low shear rates such that *Pe*, *De* ≪ 1, $\tau^a_{xy} \sim \dot{\gamma}$ and $N^a_1 \sim \dot{\gamma}^2$. The reason for this is as follows: for *De* ≪ 1, $\tau_{xy}' \sim \tau^p_{xy} \sim \dot{\gamma}$, $\tau_{xy}' \gg \tau_{xx}'$, and $\tau^a_{ij} \cong \tau^a_{kk}{}^{\circ}(\delta_{ij}/3)$. By balancing the *xy* component of the diffusion and stress-enhancement terms of eq 57 to lowest order in $\dot{\gamma}$, one obtains

$$\tau^a_{xy}\tau^a_{kk} \sim \frac{1}{\Xi}\tau^a_{xx}\tau^a_{yy}\tau_{xy}' \quad \text{and} \quad \tau^a_{xy} \sim \frac{De}{\Xi\alpha} \tag{70}$$

Balancing the largest *xx*- and *yy*-components of eq 57 for *Pe*, *De* ≪ 1,

$$N^a_1\tau^a_{kk} \sim \frac{1}{\Xi}(\tau^a_{xx})^2\tau_{xx}' \quad \text{and} \quad N^a_1 \sim \frac{2De^2}{\Xi\alpha} \tag{71}$$

as seen in Figure 2. The effect of decreasing the osmotic pressure (i.e., decreasing Ξ) is to increase the magnitude of the anomalous stress as seen in Figures 1 and 2. This is because concentration fluctuations are more readily altered from their average equilibrium isotropic state as the system becomes more compressible. As an aid in the interpretation of the results, the angle of orientation of the anomalous stress principal axis $\chi^a \equiv {}^1/_2\,\text{atan}(2\tau^a_{xy}/N^a_1)$ and the polymer stress axis $\chi^p$ are shown in Figure 3. In the limit of zero shear rate, $\chi^p = 45°$ and $\chi^a = 135°$ and the structure factor in the $x-y$ plane is a butterfly pattern with its two high intensity peaks positioned on the $k_x = k_y$ axis. With increasing shear rate $\dot{\gamma}$, normal stresses become increasingly important in the polymer rheology, and $\chi^p$ decreases from 45°

toward 0°. If the effect of convection is not taken into account, the principal axes of $\tau^a$ and the fluctuating polymeric stress $\delta\tau^p$ are perpendicular to each other and the angle of the anomalous stress axis then correspondingly decreases from 135°. This behavior corresponds to a rotation of the butterfly pattern toward the $k_x$ axis as has been observed experimentally.[12,13] With increasing shear rate, the difference between $\chi^a$ and $\chi^p$ decreases due to deformation and elongation along the flow direction by convection of concentrated regions. Polymeric stress shear thins at shear rates such that $De > 1$, while convection remains linear in $\dot{\gamma}$. Hence, convection becomes increasingly important relative to stress enhancement with increasing shear rate and $\tau^a_{xy}$ decreases in magnitude. At $Pe \cong 2$, $\chi^a = 90°$ and $\tau^a_{xy} = 0$. Above $Pe \cong 2$, $\chi^a < 90°$ and $\tau^a_{xy}$ becomes positive and therefore causes an increase in the overall shear stress $\tau_{xy}$. At shear rates such that $Pe > 6$, $\chi^a$ becomes less than 45° and $N_1^a$ becomes positive, thus increasing the overall normal stress $N_1^a + N_1^p$. This type of behavior can be tested experimentally using SALS and dichroism experiments. In simple shear, van Egmond *et al.*[13] have shown that the steady-state angle of anisotropic fluctuations in PS/DOP solutions follows the same trend. In Figure 3, the dichroic angle measured at 16 °C is superimposed on predicted angles. In calculating the Peclet number, a diffusive time scale $t_D = 1.0$ s was chosen.

In addition to the change in sign of the anomalous stress contributions, the viscosity of the anomalous stress $\tau^a_{xy}/\dot{\gamma}$ shear-thickens when it is positive. $\tau^a_{xy}$ is also at least an order of magnitude greater when it is positive than when it is negative. Therefore, when the polymeric and anomalous contributions to the stress are of the same order of magnitude, the fluid can display overall shear thickening behavior. As seen in Figure 1, the value of $Pe$ where $\tau^a_{xy}$ becomes positive is approximately constant, but the magnitude of $\tau^a_{xy}$ at any given $Pe$ increases strongly with decreasing $\Xi$, so shear thickening becomes more pronounced as temperature approaches the coexistence curve. Indeed, there is experimental evidence in the literature for this effect. As mentioned in the Introduction, Yanase *et al.* observed shear thickening in PS/DOP below its $\theta$ temperature (22 °C) and ascribed this effect to shear-induced structure and found it to be most pronounced at the lowest temperatures.[11] Since the characteristic polymeric and diffusive time for PS/DOP increases with decreasing temperature in the range $T = 20-14$ °C, the shear rate at which convection dominates and $\tau_{xy}$ shear-thickens decreases.[13] The critical Deborah number for shear thickening in this system was measured by Moldenaers *et al.*[27] to be $De_c \cong 5$, which corresponds roughly to predicted shear rates where $\tau^a_{xy}$ becomes large and positive. In addition, shear thickening was observed to occur only at shear rates above which polymeric stress becomes shear thinning.[11,27] This is in agreement with the mechanism for shear thickening by convection-dominated enhancement described above.

Since the study of shear-induced phase separation was first observed by a flow-induced turbidity, we present values for the integrated structure factor (i.e., $Q$), which should be proportional to turbidity. As can be seen in Figure 4, $Q$ increases with increasing shear rate. This same trend has also been observed in PS/DOP.[11,30] Further, for any given shear rate, $Q$ increases with decreasing $\Xi$ because of the increasing compressibility of the system with decreasing $\chi^{-1}$. Above a certain shear rate, $Q$ decreases with increasing shear rate. At shear rates above $Pe \cong 5$, $Q$ drops below its quiescent value. This effect is due to the increase and change of sign of $N_1^a$, which causes the stress-enhancement term in eq 60 to decrease $Q$. A shear-induced decrease of scattering intensity has been observed by Hashimoto and co-workers[15,16] in ternary PS/PB/DOP solutions that undergo flow-induced mixing. For this system, a streaklike scattering pattern oriented perpendicular to the flow direction is observed. The overall scattering along the $k_x$ axis is strongly suppressed and the overall intensity decreases. This type of pattern corresponds to positive $N_1^a$ and so is consistent with the model.

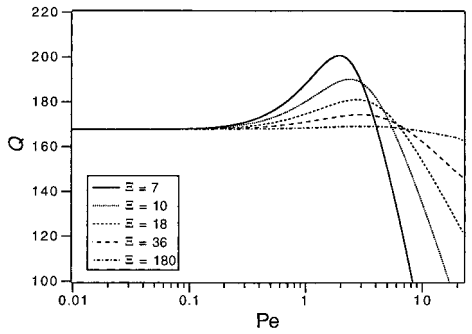


**Figure 4.** Steady-state integrated structure factor, $Q$, as a function of $Pe$, for a range of $\Xi$.

**VIIIB. Time-Dependent Behavior.** The time dependent response of $\tau^a_{xy}$ to inception and cessation of shear flow for a range of low shear rates $Pe = 0.2-0.7$ is shown in Figure 5a. At the lowest shear rates, $\tau^a_{xy}$ approaches its negative steady state monotonically. However, as convection becomes increasingly important, negative overshoots become apparent both on approach to steady state and on flow cessation. The first overshoot occurs because of growth of $\tau^a_{xy}$ by stress enhancement, followed by reduction in $\tau^a_{xy}$ by convection. Initially, convection can have no effect on anomalous stress when $\tau^a_{ij}$ is isotropic (see the form of eq 57). Furthermore, since the time scales are similar, convection, stress enhancement, and diffusion affect $S(\mathbf{k})$ at similar rates. On flow cessation, the effect of convection is rapidly removed. However, since polymeric stress decays slowly, residual polymer stress still couples to concentration fluctuations, thus causing an initial increase in negative $\tau^a_{xy}$ before decay to isotropy. Both overshoots in structure formation were observed by Yanase *et al.*[11] using scattering dichroism measurements in the $x-z$ plane and by van Egmond *et al.*[13] and Migler *et al.*[30] using small-angle light scattering in the $x-y$ plane. In these studies, the overshoot on flow cessation was attributed to a "stress recoil" effect. Similar overshoots have also been observed by SALS in wormlike micelle solutions.[54] The response of $\tau^a_{xy}$ at moderate shear rates ($Pe = 1.0-2.0$) is plotted as a function of time in Figure 5b. The steady-state value of the shear component becomes increasingly positive as a result of the increased effect of convection relative to that of stress enhancement. After flow inception, a positive overshoot that follows the first negative overshoot becomes increasingly pronounced with increasing shear rate. This extra positive overshoot is the result of the startup transient given by the lower convected derivative when the shear rate is greater than the inverse diffusive relaxation time $\tau_D$. In eq 57, the

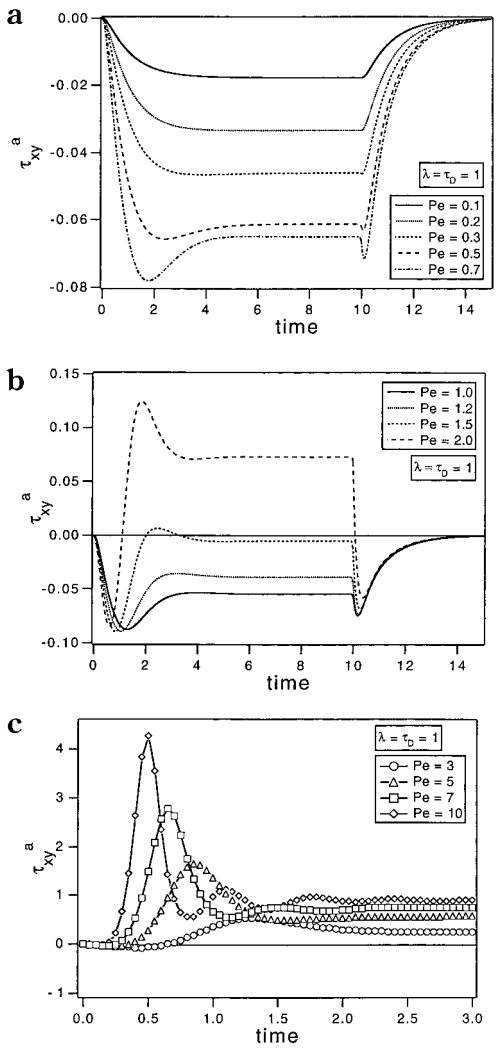


**Figure 5.** Time-dependent response of $\tau_{xy}^a$ to simple shear flow at (a) $Pe = 0.1, 0.2, 0.3, 0.5, 0.7$, (b) $Pe = 1.0, 1.2, 1.5, 2.0$, and (c) $Pe = 3, 5, 7, 10$.

convected derivative contains the convection term, and so the overshoot becomes apparent when convection becomes important. The height of the positive overshoot relative to the steady-state value of $\tau_{xy}^a$ increases dramatically with increasing shear rate as can be seen in Figure 5c, depicting the birefringence response for the first 3.0 s after shear inception.

The transient response of the first normal stress $N_1^a$ is plotted for various shear rates in Figure 6 and follows similar trends as seen for $\tau_{xy}^a$. Note the change in time scale between these two figures. These include the negative overshoots after flow inception and cessation and the development of the positive overshoot when $N_1^a$ becomes positive and is convection dominated. However, $N_1^a$ becomes positive at a higher shear rate ($Pe \cong 6$) than that for $\tau_{xy}^a$.

**VIIIC. Dichroism Measurements.** To qualitatively test the relation between dichroism and anomalous stress, experiments in simple shear flow where conducted on a semidilute polymer solution that is known to undergo shear-enhanced scattering. Our sample consisted of a solution of PS ($M_W = 1.86 \times 10^6$) in DOP with a volume fraction, $\phi^\circ = 0.06$. The solution was prepared in the same way as in ref 13. The characteristic rheological time scale $\lambda = 1.0$ s was determined by fitting a single exponential decay to the

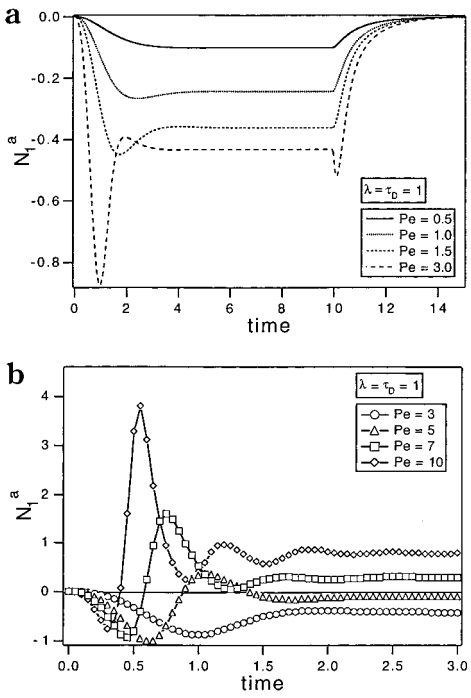


**Figure 6.** Time-dependent response of $N_1^a$ to simple shear flow at (a) $Pe = 0.5, 1.0, 1.5, 2.0$ and (b) $Pe = 3, 5, 7, 10$.

birefringence relaxation after shear cessation. Recently the relaxation time of a similar system after shear cessation has also been measured by using light scattering.[80] The solution has a $\theta$ temperature of 22 °C and a cloud point of 11 °C. Experiments were conducted at 16 °C in a standard rheo-optical train configured with a rotating half-wave plate to provide polarization modulation for measuring time-dependent dichroism.[78] A concentric cylinders Couette flow cell with a path length of 2.5 cm and a gap of 2 mm was driven by a Compumotor stepping motor to provide precise shear flow profiles.

Measurements of $\Delta n''$ and $\chi''$were conducted in shear flow in the $x-y$ plane. From eq 62, $n_{xy}''$ and $N_1''$ were calculated. In Figure 7a, the time dependent response of $n_{xy}''$ is shown for shear rates 0.5, 1, 2, and 5 $s^{-1}$. The trends are similar to the predicted response of $\tau_{xy}^a$. The steady-state value becomes increasingly negative at the two lowest shear rates. When the shear rate is increased to 2 $s^{-1}$, $n_{xy}''$ becomes less negative and becomes positive at $\dot{\gamma} = 5$ $s^{-1}$. After flow inception, $n_{xy}''$ monotonically reaches a negative steady state at a low shear rate of 0.5 $s^{-1}$. As shear rate is increased, a negative overshoot appears, and at the highest shear rate of $\dot{\gamma} = 5$ $s^{-1}$, a second positive overshoot becomes evident. On flow cessation, the relaxation behavior is also similar to predictions: the negative overshoot becomes increasingly prominent with increasing shear rate. The time-dependent behavior of $N_1''$ is less dramatic for the shear rates investigated (see Figure 7b). As expected, the steady-state value of $N_1''$ becomes increasingly negative as shear rate is increased. $N_1''$ displays neither a minimum nor a sign changes over the same range of shear rates for $n_{xy}''$ in Figure 7a. As shown in Figures 1 and 2, that the sign change occurs at higher shear rates for $N_1^a$ than $\tau_{xy}^a$ conforms with model predictions. At $\dot{\gamma} = 2$ $s^{-1}$, $N_1''$ undergoes a negative overshoot on shear inception, and at $\dot{\gamma} = 5$ $s^{-1}$, an additional overshoot on cessation appears, again in agreement with the trends in Figure 6a. Dichroism measurements at higher shear rates were increasingly difficult because

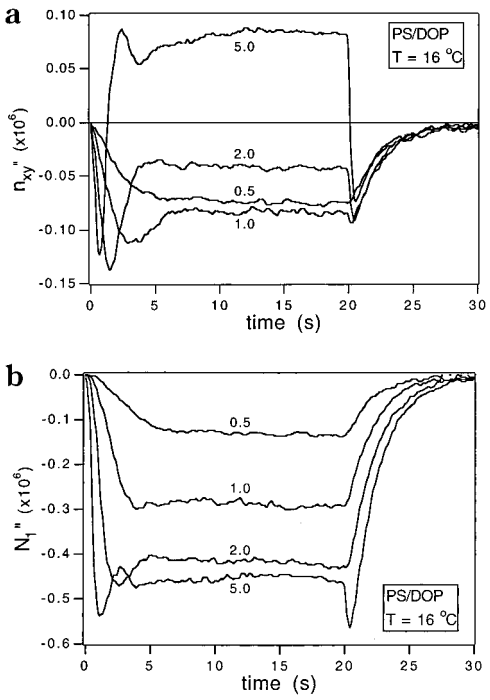


**Figure 7.** Time-dependent response of (a) $n_{xy}''$ and (b) $n_x''-n_{yy}''$ to simple shear flow of 6 wt % PS/DOP at various shear rates; $T = 16$ °C. Numbers on the plot indicate shear rate in $s^{-1}$.

of multiple scattering and highly attenuated beam intensity.

**VIIID. Second Stress Overshoot.** At this stage quantitative comparison of the model developed above with experimental results is probably inappropriate because of the approximations introduced in the model as well as due to uncertainties in the values of osmotic pressure, concentration dependence of viscosity, and relaxation time. However, if predicted trends are in agreement with experimental observation, we can gain a certain amount of confidence about the general validity of the model. As mentioned above, Yanase *et al.* and others have observed shear thickening in entangled polymers in poor solvent at the same shear rates as shear-induced structures develop as measured by dichroism and SALS. As predicted, shear thickening occurs at lower shear rates when the temperature approaches the coexistence curve in poor solutions. Another interesting phenomenon recently observed by Magda *et al.*[60] and Kume *et al.*[26] is the appearance of a second overshoot in both mechanical shear and first normal stress in entangled PS/DOP solutions. The first overshoot is an entanglement effect due to the instantaneous deformation of entangled polymer chains and their subsequent relaxation. The second overshoot is generally attributed to a growth of shear-induced structures, but was poorly understood. This second overshoot only occurs at high shear rates and its magnitude increases as temperature is decreased toward the coexistence temperature. These two conditions suggest that the second overshoot is related to positive transients in the anomalous stress and can be explained as follows. If the polymer relaxation time is smaller than the characteristic diffusive time ($\lambda < \tau_D$), the predicted positive overshoot in the anomalous stress (see Figures 5c and 6b) occurs after the polymer stress overshoot and so manifests itself as a second overshoot in the overall mechanical stress. Moreover, both Magda *et al.* and Kume *et al.* observed a minimum in stress between the two overshoots that is much lower than the steady state reached after the second overshoot. This may be because the anomalous stress does not add to the overall stress before the second overshoot. In fact, the anomalous stress itself undergoes a negative overshoot before the positive overshoot. It should be possible to correlate the second overshoot in the stress with corresponding changes in the shear-induced structure as measured by dichroism or SALS. Generally, Kume *et al.* found that scattering patterns changed from a butterfly pattern oriented along the flow direction to a streak oriented perpendicular to the flow direction at shear rates where the second stress overshoot appears and the system becomes shear thickening. However, when comparing the orientation and anisotropy of SALS patterns with shear and first normal stress overshoots, it is important to be careful of the plane of measurement. In the work of Kume *et al.*, scattering experiments were done in the $x-z$ plane, and so it is not possible to rigorously compare stress overshoots with structure formation in the $x-y$ plane.

Polymer solutions are not the only systems to display a second stress overshoot. Very recently, a second shear stress overshoot was observed by Kadoma and van Egmond in wormlike micelle solutions that undergo shear-enhanced scattering.[54] The time at which the overshoot occurs is comparable to the overshoot in scattering anisotropy, and the shear rate corresponds roughly to the shear rate at which the scattering anisotropy changes sign, indicating that the anomalous stress is positive. In these studies, scattering was again unfortunately only measured in the $x-z$ plane.

The possibility for other types of time-dependent phenomena exists. Polymeric stresses are known to cause purely elastic instabilities that are characterized by the appearance of secondary flows.[81] In systems that undergo strong shear induced scattering, there is a possibility of fluid mechanical instabilities caused primarily by anomalous stresses. This is particularly true when the anomalous stress dominates the polymeric stress, as in the shear-thickening region. Such an instability could be rooted in the dynamic competition between diffusional, stress-enhancement, and convective mechanisms. In fact, scattering dichroism has been observed to fluctuate rapidly in the shear-thickening regime of PS/DOP solutions.[11]

## IX. Conclusion

A model describing the evolution of the anomalous stress in poor polymer solutions has been developed. The predictions of the model in simple shear flow have been shown to be in qualitative agreement with many of the steady state and time dependent phenomena observed experimentally. These phenomena include shear thickening and the second overshoot in the shear stress. A stress−optic rule has also been developed to describe the relationship between dichroism and anomalous stress.

Quantitative comparison of model predictions with experimental results is still not really possible because of the many approximations introduced in deriving eq 57. These approximations include the neglect of velocity fluctuations, slaving the stress to the concentration fluctuations, various decoupling approximations, and perhaps most importantly, the somewhat arbitrary choice of $\Lambda = 2$.

The methodology developed in this paper can be applied to a large number of problems involving the

rheological effect of flow-modified structure in complex fluids including textured liquid crystals, block copolymers, and phase-separated blends. It is also possible that the anomalous stress may play an important role in driving fluid mechanical instabilities in various systems.

**Acknowledgment.** This work was made possible through a grant from the MRSEC program at the University of Massachusetts, Amherst (NSF/DMR-9400488).

## References and Notes

(1) Rangel-Nafaile, C.; Metzner, A.; Wissbrun, K. *Macromolecules* **1984**, *17*, 1187.
(2) Larson, R. G. *Rheol. Acta* **1992**, *31*, 497.
(3) Ver Strate, G.; Philippoff, W. J. *Polym. Sci., Polym. Lett.* **1974**, *12*, 267.
(4) Wolf, B. A. *Macromolecules* **1984**, *17*, 615. Kramer-Lucas, H.; Schenck, H.; Wolf, B. A. *Makromol. Chem.* **1988**, *189*, 1627. Horst, R.; Wolf, B. A. *Rheol. Acta* **1994**, *33*, 99.
(5) Brochard, F.; de Gennes, P.-G. *Macromolecules* **1977**, *10*, 1157. Brochard, F. *J. Phys. (France)* **1983**, *44*, 39.
(6) Adam, M.; Delsanti, M. *Macromolecules* **1985**, *18*, 1760.
(7) Helfand, E.; Fredrickson, G. H. *Phys. Rev. Lett.* **1989**, *62*, 2468.
(8) Onuki, A. *J. Phys. Soc. Jpn.* **1990**, *59*, 3423.
(9) Doi, M.; Onuki, A. *J. Phys. II* 1992, *2*, 1631.
(10) Milner, S. T. *Phys. Rev. Lett.* 1991, *66*, 1477.
(11) Yanase, H.; Moldenaers, P.; Abetz, V.; van Egmond, J. W., Fuller, G. G. *Rheol. Acta* **1991**, *30*, 89.
(12) Wu, X.-L.; Pine, D. J.; Dixon, P. K. *Phys. Rev. Lett.* **1991**, *66*, 2408.
(13) van Egmond, J. W.; Werner, D. E.; Fuller, G. G. *J. Phys. Chem.* **1992**, *96*, 7742.
(14) van Egmond, J. W.; Fuller, G. G. *Macromolecules* **1993**, *26*, 7182.
(15) Takebe, T.; Takeji, S.; Hashimoto, T. *J. Chem. Phys.* **1989**, *91*, 4369.
(16) Fujioka, K.; Takebe, T.; Hashimoto, T. *J. Chem. Phys.* **1993**, *98*, 717.
(17) Hashimoto, T.; Fujioka, K. *J. Phys. Soc. Jpn.* **1991**, *60*, 356.
(18) Hashimoto, T.; Kume, T. *J. Phys. Soc. Jpn.* **1992**, *61*, 1839.
(19) Hammouda, B.; Nakatani, A. I.; Waldow, D. A.; Han, C. C. *Macromolecules* **1992**, *25*, 2903.
(20) Nakatani, A.; Douglas, J.; Ban, Y.; Han, C. *J. Chem. Phys.* **1994**, *100*, 3224.
(21) Mani, S.; Malone, M. F.; Winter, H. H. *Macromolecules* **1992**, *25*, 5671.
(22) Kishbaugh, A. J.; McHugh, A. J. *Rheol. Acta* **1993**, *32*, 9; **1993**, *32*, 115.
(23) Moses, E.; Kume, T.; Hashimoto, T. *Phys. Rev. Lett.* **1994**, *72*, 2037.
(24) Murase, H.; Kume, T.; Hashimoto, T.; Ohta, Y.; Mizukami, T. *Macromolecules* **1995**, *28*, 7724.
(25) Kume, T.; Hashimoto, T. In *Flow Induced Structure in Polymers*; Nakatani, A. I., Dadmun, M. D., Eds.; American Chemical Society: Washington, DC, 1995.
(26) Kume, T.; Hattori, T.; Hashimoto, T. *Macromolecules* **1997**, *30*, 427.
(27) Moldenaers, P.; Yanase, H.; Mewis, J.; Fuller, G. G; Lee, C.-S.; Magda, J. J. *Rheol. Acta* **1993**, 32, 1.
(28) Fuller, G. G.; van Egmond, J. W.; Wirtz, D.; Peuvrel-Disdier, E.; Wheeler, E.; Takahashi, H. In *Flow Induced Structure in Polymers*; Nakatani, A. I., Dadmun, M. D., Eds.; American Chemical Society: Washington, DC, 1995.
(29) Wirtz, D. *Phys. Rev. E* **1994**, *50*, R1755.
(30) Migler, K.; Liu, C.-H; Pine, D. J. *Macromolecules* **1996**, *29*, 1422.
(31) Milner, S. T. *Phys. Rev. E* **1993**, *48*, 3674.
(32) Ji, H.; Helfand, E. *Macromolecules* **1995**, *28*, 3869.
(33) de Gennes, P.-G., *Macromolecules* **1976**, *9*, 587; **1976**, *9*, 594.
(34) Fixman, M. *J. Chem. Phys.* **1962**, *36*, 310.
(35) Sallavanti, R.; Fixman, M. *J. Chem. Phys.* **1968**, *48*, 5326.
(36) Yamada, T.; Kawasaki, K. *Progr. Theor. Phys.* **1976**, *38*, 1031.
(37) Oxtoby, O. W. *J. Chem. Phys.* **1975**, *62*, 1463.
(38) Onuki, A. *Phys. Lett.* **1977**, *64*, 115.
(39) Fredrickson, G. H. *J. Chem. Phys.* **1986**, *85*, 5306.
(40) Fredrickson, G. H.; Larson, R. G. *J. Chem. Phys.* **1987**, *86*, 1553. Larson, R. G.; Fredrickson, G. H. *Macromolecules* **1987**, *20*, 1897.
(41) Onuki, A. *Phys. Rev. A* **1987**, *35*, 5149.
(42) Ajji, A.; Choplin, L. *Macromolecules* **1991**, *24*, 5221.
(43) Kapnistos, M.; Hinrichs, A.; Vlassopoulos, D.; Anastasiadis, S. H.; Stammer, A.; Wolf, B. A. *Macromolecules* **1996**, *29*, 7155.
(44) Peterlin, A.; Turner, D. *Nature* **1963**, *197*, 488.
(45) Layec-Raphalen, M. N.; Wolff, C. *J. Non-Newtonian Fluid Mech.* **1976**, *1*, 159.
(46) Vrahopoulou, E. P.; McHugh, A. J. *J. Non-Newtonian Fluid Mech.* **1987**, *25*, 157.
(47) Wolff, C. *Adv. Colloid Interface Sci.* **1982**, *17*, 263.
(48) Dupuis, D.; Wolff, C. *J. Rheol.* **1993**, *37*, 587.
(49) Dupuis, D.; Lewandowski, F. Y.; Steiert, P.; Wolff, C. *J. Non-Newtonian Fluid Mech.* **1994**, *54*, 11.
(50) Hatzikiriakos, S. G.; Vlassopoulos, D. *Rheol. Acta* **1996**, *35*, 274.
(51) Jian, T.; Vlassopoulos, D.; Fytas, G.; Pakula, T.; Brown, W. *Colloid Polym. Sci.* 1996, *274*, 1033.
(52) Wheeler, E. K.; Izu, P.; Fuller, G. G. *Rheol. Acta* **1996**, *35*, 139.
(53) Kadoma, I. A; van Egmond, J. W. *Phys. Rev. Lett.* **1996**, *76*, 4432; *Rheol. Acta* **1997**, *36*, 1.
(54) Kadoma, I. A.; van Egmond, J. W. *Langmuir* **1997**, *13*, 4551.
(55) Osaki, K.; Inoue, T.; Ahn, K. H. *J. Non-Newtonian Fluid Mech.* **1994**, *54*, 109. Ahn, K. H.; Osaki, K. *J. Non-Newtonian Fluid Mech.* **1994**, *55*, 215.
(56) Young, A. M.; Higgins, J. S.; Peiffer, D. G.; Rennie, A. R. *Polymer* **1995**, *36*, 691. Young, A. M.; Timbo, A. M.; Higgins, J. S.; Peiffer, D. G.; Lin, M. Y. *Polymer* **1996**, *37*, 2701.
(57) Koike, A.; Nemoto, N.; Inoue, T.; Osaki, K. *Macromolecules* **1995**, *28*, 2339. Nemoto, N.; Koike, A.; Osaki, K. *Macromolecules* **1996**, *29*, 1445.
(58) Gast, A. P. *Langmuir*, **1996**, *12*, 4060.
(59) Sato, T.; Watanabe, H.; Osaki, K. *Macromolecules* **1996**, *29*, 3881.
(60) Magda, J. J.; Lee, C.-S.; Muller, S. J.; Larson, R. G. *Macromolecules* **1993**, *26*, 1696.
(61) Felderhof, B. U. *Physica* **1970**, *48*, 541.
(62) Onuki, A.; Kawasaki, K. *Phys. Lett. A* **1980**, *75*, 485.
(63) Onuki, A. *J. Phys. Soc. Jpn.* **1988**, *57*, 699.
(64) Doi, M. In *Dynamics and Patterns in Complex Fluids*; Onuki, A., Kawasaki, K., Eds.; Springer-Verlag: Berlin, 1990.
(65) Siggia, E. D.; Halperin, B. I.; Hohenberg, P. C. *Phys. Rev. B* **1976**, *13*, 2110.
(66) Batchelor, G. K. *J. Fluid Mech.* **1970**, *41*, 545.
(67) Doi, M.; Ohta, T. *J. Chem. Phys.* **1991**, *95*, 1242.
(68) Onuki, A. *Europhys. Lett.* **1994**, *28*, 175.
(69) Cahn, J. W.; Hilliard, J. E. *J. Chem. Phys.* **1958**, *28*, 258. Cook, H. E. *Acta Metall.* **1970**, *18*, 297.
(70) de Gennes, P.-G. *J. Chem. Phys.* **1980**, *72*, 4756.
(71) Binder, K. *J. Chem. Phys.* **1983**, *79*, 6387.
(72) Chakrabarti, A.; Toral, R.; Gunton, J. D.; Muthukumar, M. *J. Chem. Phys.* **1990**, *92*, 6899.
(73) Kawasaki, K.; Koga, T. *Physica A* **1993**, *201*, 115.
(74) Larson, R. G. *Constitutive Equations for Polymer Melts and Solutions*; Butterworths: Boston, 1988.
(75) Kalogrianitis, S. G.; van Egmond, J. W. *J. Rheol.* **1997**, *41*, 343.
(76) Doi, M.; Edwards, S. F. *The Theory of Polymer Dynamics*; Oxford University Press: Oxford, 1986.
(77) Truesdell, C.; Noll, W. *The Non-linear Field Theories*; Springer-Verlag: Berlin, 1965.
(78) Fuller, G. G. *Optical Rheometry of Complex Fluids*; Oxford University Press: Oxford, 1995.
(79) Onuki, A.; Doi, M. *J. Chem. Phys.* **1986**, *85*, 1190.
(80) Stepanek, P.; Brown, W.; Hvidt, S. *Macromolecules* **1997**, *29*, 8888.
(81) Larson, R. G. *Rheol. Acta* **1992**, *31*, 213.

MA9706891